Higher order (A+E)⊗e pseudo-Jahn–Teller coupling

Wolfgang Eisfeld, Alexandra Viel

Higher order $(A+E)\otimes e$ pseudo-Jahn–Teller coupling

Wolfgang Eisfeld[a)]
Lehrstuhl für Theoretische Chemie, Department Chemie, Technische Universität München, D-85747 Garching, Germany

Alexandra Viel[b)]
LPQ-IRSAMC, Université Paul Sabatier, 118 route de Narbonne, F-31062 Toulouse, France

(Received 3 December 2004; accepted 17 March 2005; published online 25 May 2005)

The pseudo-Jahn–Teller (PJT) coupling of a nondegenerate state A with a twofold degenerate state E by a degenerate vibrational mode e is studied for a general system with a C_3 main rotational axis. The PJT coupling terms up to sixth order are derived by symmetry considerations for this general $(A+E)\otimes e$ case. The obtained expression for the 3×3 diabatic potential energy matrix is found to be closely related to the expression recently developed for the higher order Jahn–Teller case [A. Viel and W. Eisfeld, J. Chem. Phys. **120**, 4603 (2004)]. The dynamical PJT coupling, which can arise for states of appropriate symmetry if one of the vibrational modes induces a change of the nuclear point group between D_{3h}, C_{3v}, C_{3h}, and C_3, is discussed. The effect of the higher order PJT coupling is tested by a two-dimensional model study based on the e bending mode of NH_3^+. The models are analyzed by fitting the two-dimensional potential energy surfaces. The significance of the higher order terms on the nonadiabatic dynamics is demonstrated by quantum wave packet propagations. © *2005 American Institute of Physics*. [DOI: 10.1063/1.1904594]

I. INTRODUCTION

Vibronic coupling, i.e., the interaction of energetically close-lying electronic states, induced by the vibrational motion of the nuclei, often plays a very important role in spectroscopy and nuclear dynamics. This is particularly true for radicals, which are usually characterized by a high density of electronic states, and molecules with high symmetry, resulting in multiply degenerate states. Such vibronic interactions can induce nonadiabatic transitions among electronic states and thus may have a strong influence on the time evolution of the system.[1,2] A prominent example of such an interaction is the well-known Jahn–Teller (JT) effect.[3,4] In this case, the symmetry-induced degeneracy of an electronic state is lifted by distortions along modes of the appropriate symmetry and thus a conical intersection is formed. A conical intersection is characterized by the breakdown of the Born–Oppenheimer (BO) approximation because the adiabatic wave functions of the interacting states cease to be continuously differentiable functions with respect to the nuclear coordinates and the symmetry point constitutes a pole of the nonadiabatic coupling elements.[5]

However, even without the existence of a conical intersection the BO approximation may be invalid if two states become sufficiently close in energy and the nonadiabatic coupling elements become large. Besides the countless cases of general avoided crossings, the so-called pseudo-Jahn–Teller effect (PJT) is particularly interesting for analyzing such nonadiabatic interactions. The PJT interaction is characterized by a degenerate mode, coupling a degenerate with a nondegenerate electronic state.[1,6–9] Such a situation can arise for any molecule with a main rotational axis C_n with $n\geqslant3$. In the present study, the case of $n=3$ is investigated.

For the theoretical treatment of the nonadiabatic dynamics of PJT systems, it is beneficial to change to the diabatic representation of the electronic states.[10,11] Although it was shown to be impossible to uniquely define strictly diabatic states,[12,13] in practice a large number of diabatization schemes has been developed and successfully applied.[14–19] Due to the high symmetry of the PJT problem, a "diabatization by ansatz" is particularly efficient and will be used throughout this study. The elements of the diabatic potential matrix are expanded as simple Taylor series of properly symmetrized nuclear coordinates and group theory is used to determine general relations of the expansion coefficients. The diabatic and adiabatic potential matrices are related by the unitary transformation that diagonalizes the diabatic matrix. Thus, the parameters of the diabatic matrix can be obtained by fitting its eigenvalues to the adiabatic energies which are available, e.g., from *ab initio* calculations.

Such an approach, which usually includes only the first (sometimes also the second) nonvanishing coupling terms, is widely used for the treatment of JT and PJT problems (see, e.g., Ref. 1 for an overview). From the dynamical point of view, the limitation to second-order terms along with using harmonic oscillator basis sets for the nuclear motion has the advantage that all terms of the Hamilton matrix can be evaluated analytically. However, the disadvantage is that for systems displaying strong anharmonicity this method will give poor results for properties determined by more extended regions of the potential energy surfaces. Zgierski and Pawlikowski already noticed that for systems with both JT

a)Electronic mail: wolfgang.eisfeld@ch.tum.de
b)Present address: PALMS-SIMPA, UMR 6627 du CNRS, Université de Rennes 1, Campus de Beaulieu, F-35042 Rennes, France; Electronic mail: alexandra.viel@univ-rennes1.fr

and PJT couplings, the second-order JT coupling needs to be included to obtain reasonable results when the first-order PJT coupling is considered.[8] In our previous study on the higher order JT couplings, we have shown that higher order couplings can have a drastic effect on the time evolution of such a system.[20] This suggests that higher order PJT coupling may also make significant contributions, particularly if higher order JT coupling is included.

The aim of the present study is to derive the higher order PJT coupling terms as was previously undertaken for the JT case. The method to determine the form of the coupling elements is based on the crude adiabatic approximation by Longuet-Higgens[21] and was already used in the previous work on the JT couplings.[20] An alternative approach, based on the same fundamental considerations, was recently outlined by Köppel.[22]

II. SYMMETRY CONSIDERATIONS

In the following, the diabatic potential matrix for the $(A+E)\otimes e$ pseudo-Jahn–Teller system up to sixth order is derived for a general molecule with a C_3 main rotational axis. Some general symmetry properties of the corresponding point groups D_{3h}, C_{3v}, C_{3h}, and C_3 with respect to JT and PJT coupling are outlined in the following.

Common to systems of all four point groups are nuclear coordinates belonging to a doubly degenerate vibrational mode e and doubly degenerate electronic states E. The invariance of the total Hamiltonian under all symmetry operations of the point group along with simple application of group theory leads to selection rules for the possible coupling patterns. Thus it can be shown that only the two components of an e mode can couple the two components of a doubly degenerate E state (JT coupling). It is also easily seen that motion along a set of e coordinates is necessary to couple a nondegenerate A state with an E state (PJT coupling).

While for the C_3 group these are the only rules (because there is no distinction between different A and E representations) for C_{3v} and D_{3h} further considerations apply. The six irreducible representations of the D_{3h} group are A_1', A_2', E', A_1'', A_2'', and E''. It follows that the components of an E' (or E'') state can be coupled by an e' mode in any order but only by even orders of an e'' set of coordinates. For PJT coupling a similar pattern is obtained. A_1' and A_2' states can interact with an E' state by any order in an e' coordinate and by even orders in an e'' mode. The same is true for interactions between A_1'' and A_2'' states with an E'' state. In contrast, for coupling of A_1' and A_2' states with an E'' state coupling can only occur by odd orders in an e'' mode. This is also true for an interaction between A_1'' and A_2'' states with an E' state.

The rules given above have to be modified when more than one vibrational mode is taken into account. A particularly frequent example is when an a_1'' or a_2'' coordinate is physically relevant. In this case, the PJT coupling between pairs of states $A'_{(1,2)}/E''$ or $A''_{(1,2)}/E'$, respectively, will strongly depend on the $a''_{(1,2)}$ coordinate (dynamical PJT coupling). Such a situation is analyzed in more detail in Sec. III B 3.

The degeneracy of the E state means that there exist two linearly independent eigenvectors $|\Psi_1\rangle$ and $|\Psi_2\rangle$ associated to the same eigenvalue of the electronic Hamiltonian. Any arbitrary, normalized linear combination of these two vectors will again be an eigenvector to the same eigenvalue. This fact will be utilized in the following. However, in the D_{3h} and C_{3v} cases, there exist two particular linear combinations $|\Psi_x\rangle$ and $|\Psi_y\rangle$, which transform like different irreducible representations of the subgroups C_{2v} (D_{3h}) or C_s (C_{3v}).

III. $(A+E)\otimes e$ PSEUDO-JAHN–TELLER EFFECT

A. Complex representation

The invariance of the total Hamiltonian under the symmetry operations of the symmetry point group of the system is used to obtain the nonvanishing terms of the potential energy matrix. The complex representation for both the vibrational degrees of freedom and the electronic states simplifies the study of the effect of the $\hat{C}_3$ symmetry operator. A set of complex coordinates, corresponding to the e vibrational mode, is obtained from the real coordinates x and y by the transformation,

$$Q_+ = x + iy, \tag{1a}$$

$$Q_- = x - iy. \tag{1b}$$

The two orthogonal components of the electronically degenerate E state ($\langle\Psi_1|$ and $\langle\Psi_2|$) are modified by the corresponding unitary transformation whereas the nondegenerate electronic eigenfunction ($\langle\Psi_a|$) remains unaffected,

$$\mathbf{U}^\dagger \boldsymbol{\Psi}_{(a12)} = \frac{1}{\sqrt{2}}\begin{pmatrix} \sqrt{2} & 0 & 0 \\ 0 & 1 & i \\ 0 & 1 & -i \end{pmatrix}\begin{pmatrix} \langle\Psi_a| \\ \langle\Psi_1| \\ \langle\Psi_2| \end{pmatrix} = \begin{pmatrix} \langle\Psi_a| \\ \langle\Psi_+| \\ \langle\Psi_-| \end{pmatrix} = \boldsymbol{\Psi}_{(a+-)}. \tag{2}$$

In this complex representation both the coordinates Q_+, Q_- and the state functions $\langle\Psi_+|$, $\langle\Psi_-|$ are eigenfunctions of the symmetry operator $\hat{C}_3$ with eigenvalues $e^{\pm 2i\pi/3}$. In contrast, the $\langle\Psi_a|$ state function is invariant with respect to this operation. Thus, a rotation of $2\pi/3$ transforms the complex coordinates as

$$\hat{C}_3 Q_+ = e^{+2\pi i/3} Q_+, \quad \hat{C}_3 Q_- = e^{-2\pi i/3} Q_-, \tag{3}$$

and the electronic state functions as

$$\hat{C}_3\langle\Psi_a| = \langle\Psi_a|, \quad \hat{C}_3|\Psi_a\rangle = |\Psi_a\rangle, \tag{4a}$$

$$\hat{C}_3\langle\Psi_+| = e^{-2\pi i/3}\langle\Psi_+|, \quad \hat{C}_3|\Psi_+\rangle = e^{+2\pi i/3}|\Psi_+\rangle, \tag{4b}$$

$$\hat{C}_3\langle\Psi_-| = e^{+2\pi i/3}\langle\Psi_-|, \quad \hat{C}_3|\Psi_-\rangle = e^{-2\pi i/3}|\Psi_-\rangle. \tag{4c}$$

The representation of the electronic Hamiltonian in the $\{|\Psi_a\rangle, |\Psi_+\rangle, |\Psi_-\rangle\}$ basis is given by

TABLE I. Nonvanishing terms of the 3×3 Hamiltonian matrix in complex representation.

Order	Diagonal $H_{aa}=H_{++}=H_{--}$	Off-diagonal $H_{a-}=H_{+a}=H_{-+}=(H_{a+})^*=(H_{-a})^*=(H_{+-})^*$
0	$Q_+^0Q_-^0$	—
1	—	$Q_+^0Q_-^1$
2	$Q_+^1Q_-^1$	$Q_+^2Q_-^0$
3	$Q_+^3Q_-^0$ and $Q_+^0Q_-^3$	$Q_+^1Q_-^2$
4	$Q_+^2Q_-^2$	$Q_+^0Q_-^4$ and $Q_+^3Q_-^1$
5	$Q_+^4Q_-^1$ and $Q_+^1Q_-^4$	$Q_+^2Q_-^3$ and $Q_+^5Q_-^0$
6	$Q_+^6Q_-^0$ and $Q_+^3Q_-^3$ and $Q_+^0Q_-^6$	$Q_+^1Q_-^5$ and $Q_+^4Q_-^2$

$$\hat{H}_{\mathrm{el}}=\mathbf{\Psi}^{\dagger}_{(a+-)}\mathbf{H}_{(a+-)}\mathbf{\Psi}_{(a+-)}=\sum_{i,j}|\Psi_i\rangle H_{ij}\langle\Psi_j| \quad (i,j=a,+,-), \tag{5}$$

and the matrix elements $H_{ij}=\langle\Psi_i|\hat{H}_{\mathrm{el}}|\Psi_j\rangle$ $(i,j=a,+,-)$ are expanded as Taylor series up to sixth order in Q_+ and Q_-. Each term of the expansion for each element of Eq. (5) has to fulfill the invariance condition when applying the $2\pi/3$ rotation operator. For example,

$$\hat{C}_3|\Psi_a\rangle Q_+^pQ_-^q\langle\Psi_+| = 1\times e^{(+p)2\pi i/3}e^{(-q)2\pi i/3}e^{-2\pi i/3} \times|\Psi_a\rangle Q_+^pQ_-^q\langle\Psi_+| \tag{6}$$

can contribute only for (p,q) combinations which fulfill the condition $(p-q-1)(\mathrm{mod}\ 3)=0$. The nonvanishing terms of the matrix H_{ij} are given in Table I in which the Jahn–Teller terms obtained in Ref. 20 have been reported again for completeness. Note that the nonvanishing terms of the matrix element H_{a+} are the same as the ones of H_{+-}.[23]

Next, the invariance of the nonvanishing terms with respect to the other symmetry operations of the symmetry group needs to be tested. To this end, the obtained Hamiltonian matrix is transformed back to the real representation.

B. Real representation

The real representation for both the electronic state functions and the nuclear coordinates are often preferred for the *ab initio* computation of electronic energies and for the dynamics studies. The matrix representation $\mathcal{H}$ of the electronic Hamiltonian in the real representation, including all Jahn–Teller and pseudo-Jahn–Teller couplings up to sixth order, is obtained by the back transformation,

$$\hat{H}_{\mathrm{el}}=\mathbf{\Psi}^{\dagger}_{(a+-)}\mathbf{U}^{\dagger}\mathbf{U}\mathbf{H}_{(a+-)}\mathbf{U}^{\dagger}\mathbf{U}\mathbf{\Psi}_{(a+-)}=\mathbf{\Psi}^{\dagger}_{(a12)}\mathcal{H}\mathbf{\Psi}_{(a12)}. \tag{7}$$

This results in the factorized expression:

$$\mathcal{H}=\mathbf{U}\mathbf{H}\mathbf{U}^{\dagger}=\sum_{n=0}^{6}\frac{1}{n!}\left\{\begin{pmatrix}\mathcal{V}_A^{(n)}&0&0\\0&\mathcal{V}_E^{(n)}&0\\0&0&\mathcal{V}_E^{(n)}\end{pmatrix}+\begin{pmatrix}0&0&0\\0&\mathcal{W}_{\mathrm{JT}}^{(n)}&\mathcal{Z}_{\mathrm{JT}}^{(n)}\\0&\mathcal{Z}_{\mathrm{JT}}^{(n)}&-\mathcal{W}_{\mathrm{JT}}^{(n)}\end{pmatrix}+\begin{pmatrix}0&\mathcal{W}_{\mathrm{PJT}}^{(n)}&-\mathcal{Z}_{\mathrm{PJT}}^{(n)}\\\mathcal{W}_{\mathrm{PJT}}^{(n)}&0&0\\-\mathcal{Z}_{\mathrm{PJT}}^{(n)}&0&0\end{pmatrix}\right\}$$
$$=\sum_{n=0}^{6}\frac{1}{n!}\{\mathbf{V}_{\mathrm{diag}}^{(n)}+\mathbf{V}_{\mathrm{JT}}^{(n)}+\mathbf{V}_{\mathrm{PJT}}^{(n)}\}. \tag{8}$$

The diagonal matrices $\mathbf{V}_{\mathrm{diag}}^{(n)}$ represent the potentials of the corresponding states in absence of any coupling. The matrices $\mathbf{V}_{\mathrm{JT}}^{(n)}$ are responsible for the splitting of the degenerate state due to the Jahn–Teller effect whereas $\mathbf{V}_{\mathrm{PJT}}^{(n)}$ are the pseudo-Jahn–Teller coupling matrices. The explicit parametrized expressions for the diagonal $\mathcal{V}^{(n)}$ elements and the coupling elements $\mathcal{W}^{(n)}$ and $\mathcal{Z}^{(n)}$ are given by

$$\mathcal{V}^{(0)}=a_1^{(0)}, \tag{9a}$$

$$\mathcal{V}^{(1)}=0, \tag{9b}$$

$$\mathcal{V}^{(2)}=a_1^{(2)}[x^2+y^2], \tag{9c}$$

$$\mathcal{V}^{(3)}=a_1^{(3)}[2x^3-6xy^2], \tag{9d}$$

$$\mathcal{V}^{(4)}=a_1^{(4)}[x^4+2x^2y^2+y^4], \tag{9e}$$

$$\mathcal{V}^{(5)}=a_1^{(5)}[2x^5-4x^3y^2-6xy^4], \tag{9f}$$

$$\mathcal{V}^{(6)}=a_1^{(6)}[2x^6-30x^4y^2+30x^2y^4-2y^6]+a_2^{(6)}[x^6+3x^4y^2+3x^2y^4+y^6], \tag{9g}$$

$$\mathcal{W}^{(0)}=0, \tag{10a}$$

$$\mathcal{W}^{(1)}=\lambda_1^{(1)}x, \tag{10b}$$

$$\mathcal{W}^{(2)}=\lambda_1^{(2)}[x^2-y^2], \tag{10c}$$

$$\mathcal{W}^{(3)}=\lambda_1^{(3)}[x^3+xy^2], \tag{10d}$$

$$\mathcal{W}^{(4)}=\lambda_1^{(4)}[x^4-6x^2y^2+y^4]+\lambda_2^{(4)}[x^4-y^4], \tag{10e}$$

$$\mathcal{W}^{(5)}=\lambda_1^{(5)}[x^5-10x^3y^2+5xy^4]+\lambda_2^{(5)}[x^5+2x^3y^2+xy^4], \tag{10f}$$

$$\mathcal{W}^{(6)}=\lambda_1^{(6)}[x^6-5x^4y^2-5x^2y^4+y^6]+\lambda_2^{(6)}[x^6+x^4y^2-x^2y^4-y^6], \tag{10g}$$

$$\mathcal{Z}^{(0)}=0, \tag{11a}$$

$$\mathcal{Z}^{(1)}=\lambda_1^{(1)}y, \tag{11b}$$

$$\mathcal{Z}^{(2)}=-2\lambda_1^{(2)}xy, \tag{11c}$$

TABLE II. Symmetry properties of the nuclear coordinates, of the nonzero matrix elements ($n>0$ for $\mathcal{W}$ and $\mathcal{Z}$) and of the possible electronic state functions in D_{3h} symmetry.

	$\chi_{\hat{C}_2}$	$\chi_{\hat{\sigma}_v}$	$\chi_{\hat{\sigma}_h}$
$x\ (e'_x, e''_x)$	+1, −1	+1	+1, −1
$y\ (e'_y, e''_y)$	−1, +1	−1	+1, −1
$\mathcal{V}^{(n)}\ (e')$	+1	+1	+1
$\mathcal{W}^{(n)}\ (e')$	+1	+1	+1
$\mathcal{Z}^{(n)}\ (e')$	−1	−1	+1
$\mathcal{V}^{(n)}\ (e'')$	+1 (even n); −1 (odd n)	+1	+1 (even n); −1 (odd n)
$\mathcal{W}^{(n)}\ (e'')$	+1 (even n); −1 (odd n)	+1	+1 (even n); −1 (odd n)
$\mathcal{Z}^{(n)}\ (e'')$	−1 (even n); +1 (odd n)	−1	+1 (even n); −1 (odd n)
E'_x	+1	+1	+1
E'_y	−1	−1	+1
A'_1	+1	+1	+1
A'_2	−1	−1	+1
E''_x	−1	+1	−1
E''_y	+1	−1	−1
A''_1	+1	−1	−1
A''_2	−1	+1	−1

$$\mathcal{Z}^{(3)} = \lambda_1^{(3)}[x^2y + y^3], \tag{11d}$$

$$\mathcal{Z}^{(4)} = \lambda_1^{(4)}[4x^3y - 4xy^3] + \lambda_2^{(4)}[-2x^3y - 2xy^3], \tag{11e}$$

$$\mathcal{Z}^{(5)} = \lambda_1^{(5)}[-5x^4y + 10x^2y^3 - y^5] + \lambda_2^{(5)}[x^4y + 2x^2y^3 + y^5], \tag{11f}$$

$$\mathcal{Z}^{(6)} = \lambda_1^{(6)}[4x^5y - 4xy^5] + \lambda_2^{(6)}[-2x^5y - 4x^3y^3 - 2xy^5]. \tag{11g}$$

It is worth noting that the elements of the JT and PJT coupling matrices are of identical form and are only distinguished by different coupling constants $\lambda_m^{(n)}$. It now needs to be tested whether the Hamiltonian in the real representation fulfills the invariance condition with respect to the remaining symmetry operations of the nuclear point group.

1. D_{3h} Symmetry

The most restrictive rules apply in the case of D_{3h} symmetry. Besides the $\hat{C}_3$ rotation, this group is characterized by the operators $\hat{C}_2$, $\hat{\sigma}_v$, $\hat{\sigma}_h$, and $\hat{S}_3$. The $\hat{S}_3$ operator is special insofar that it corresponds to a successive application of $\hat{C}_3$ and $\hat{\sigma}_h$. However, the Hamiltonian derived in the preceding section is constructed to be invariant under the $\hat{C}_3$ operation and thus the symmetry properties with respect to $\hat{S}_3$ are fully equivalent to those with respect to $\hat{\sigma}_h$. Similarly, the $\hat{C}_2$ rotation can also be achieved by successive application of $\hat{\sigma}_v$ and $\hat{\sigma}_h$ and thus it is sufficient to test the invariance of the Hamiltonian under the latter two operations. The symmetry properties of the x and y nuclear coordinates as well as the ones resulting for the $\mathcal{V}$, $\mathcal{W}$, and $\mathcal{Z}$ functions are given in Table II. The characters for the electronic state functions are also presented in Table II. Here the fact is used that the components E'_x and E'_y can be chosen to transform as A_1 and B_2 in the subgroup C_{2v} while E''_x and E''_y transform as B_1 and A_2. The same correspondence is used for the degenerate coordinates e' and e''.

TABLE III. Nonvanishing coupling elements $\mathcal{H}_{ij}$, $i, j \in \{a, x, y\}$ in the real representation for D_{3h} symmetry. Given in parentheses are the possible order of the coupling elements for coupling by e'/e'' modes.

	E'_x	E'_y	E''_x	E''_y
A'_1	$\mathcal{W}^{(n)}$ (all/even)	$\mathcal{Z}^{(n)}$ (all/even)	$\mathcal{W}^{(n)}$ (—/odd)	$\mathcal{Z}^{(n)}$ (—/odd)
A'_2	$\mathcal{Z}^{(n)}$ (all/even)	$\mathcal{W}^{(n)}$ (all/even)	$\mathcal{Z}^{(n)}$ (—/odd)	$\mathcal{W}^{(n)}$ (—/odd)
A''_1	$\mathcal{Z}^{(n)}$ (—/odd)	$\mathcal{W}^{(n)}$ (—/odd)	$\mathcal{Z}^{(n)}$ (all/even)	$\mathcal{W}^{(n)}$ (all/even)
A''_2	$\mathcal{W}^{(n)}$ (—/odd)	$\mathcal{Z}^{(n)}$ (—/odd)	$\mathcal{W}^{(n)}$ (all/even)	$\mathcal{Z}^{(n)}$ (all/even)

For a general D_{3h} symmetric molecule there may exist coordinates of e' as well as e'' character, though in the most common examples of AB_3 molecules only e' coordinates are present. The e' and e'' sets of coordinates are distinguished by their transformation under $\hat{\sigma}_h$. It follows that for e' coordinates all orders of $\mathcal{V}$, $\mathcal{W}$, and $\mathcal{Z}$ are invariant under $\hat{\sigma}_h$ operation. In contrast, for an e'' mode only even orders of $\mathcal{V}$, $\mathcal{W}$, and $\mathcal{Z}$ are invariant while all odd orders are antisymmetric. For the $\hat{\sigma}_v$ operator there is no distinction between the e' and e'' case but it is found that $\mathcal{V}$ and $\mathcal{W}$ are invariant and $\mathcal{Z}$ changes sign under this operation.

The total Hamiltonian is invariant if each term of the form $|\Psi_i\rangle\mathcal{H}_{ij}\langle\Psi_j|$ with $i,j \in \{a,1,2\}$ is totally symmetric with respect to the operations given in Table II. Thus the imposed symmetry of the matrix elements $\mathcal{H}_{ij}$ depends on the symmetry of the electronic states involved in the coupling. It is easily seen that the condition

$$\chi(\mathcal{H}_{ij}) = \chi(\Psi_i)\chi(\Psi_j) \tag{12}$$

must be fulfilled for the $\hat{\sigma}_h$ and $\hat{\sigma}_v$ operations where the characters χ can be taken from Table II.

A first trivial result is that all diagonal elements $\mathcal{H}_{aa}$, $\mathcal{H}_{11}$, and $\mathcal{H}_{22}$ must be totally symmetric. The element $\mathcal{H}_{12}$, for which the symmetry is given by $\Gamma_{\Psi_1} \otimes \Gamma_{\Psi_2} \otimes \Gamma_{\mathcal{Z}}$, is always invariant for arbitrary assignments $\{\Psi_1, \Psi_2\} \leftrightarrow \{\Psi_x, \Psi_y\}$. The only limitation applies to coupling through an e'' mode in which case only even orders of $\mathcal{Z}^{(n)}$ are possible. For $\mathcal{H}_{a1}$ and $\mathcal{H}_{a2}$ the explicit form of the coupling elements depends on the symmetry of the A state and the assignment of $\{\Psi_1, \Psi_2\}$. The PJT coupling elements for all possible combinations of states are given in Table III. Depending on the symmetry of the coupling mode (e'/e''), certain couplings vanish or are limited to even or odd orders of the coupling functions $\mathcal{W}^{(n)}$ and $\mathcal{Z}^{(n)}$ which is also indicated in the table.

Table III along with Eq. (8) enables us to construct diabatic potential matrices for any combination of state symmetries and coupling modes which fulfill the invariance condition of the total Hamiltonian. As an example, for coupling of an A'_1 with an E' state by an e' mode it is found that the E state components have to be assigned as $|\Psi_1\rangle = |\Psi_x\rangle$ and $|\Psi_2\rangle = |\Psi_y\rangle$. All orders n are allowed which result in 32 free coupling parameters for a full sixth-order coupling matrix. If the A'_1 state is replaced by A'_2, only the assignment of $|\Psi_1\rangle$ and $|\Psi_2\rangle$ needs to be interchanged while the form of the diabatic matrix remains the same.

2. C_{3v}, C_{3h}, and C_3 symmetry

C_{3v}, C_{3h}, and C_3 are subgroups of D_{3h} for which the diabatic matrices can be easily obtained from the derivation of the D_{3h} case. In C_{3v} the only symmetry operator besides $\hat{C}_3$ is $\hat{\sigma}_v$ and the resulting irreducible representations are A_1, A_2, and E. The E_x and E_y components can be chosen to transform like A' and A'' of the subgroup C_s. Thus, the A_1/E coupling is described by the same diabatic matrix as the A_1'/E' pair of states coupled by an e' mode in D_{3h}. The coupling of A_2/E corresponds to the $(A_2'+E')\otimes e'$ case.

The C_{3h} group is characterized by the symmetry operators $\hat{C}_3$, $\hat{\sigma}_h$, and $\hat{S}_3$ which yields the four irreducible representations A', E', A'', and E''. The distinction between x and y components for the degenerate electronic states is useless because there is no operator available to decide about the assignment. Thus the coupling patterns are the same as for the C_{3v} case, neglecting the distinctions related to the subscripts 1 and 2.

In C_3, $\hat{C}_3$ is the only operator and there is no distinction between different A states. Here also no operator can discriminate between the E_x and E_y components. Again, this case is described by the same diabatic matrix as for C_{3v} symmetry, just without any reference to E_x and E_y and to the subscripts 1 and 2.

3. D_{3h} symmetry and dynamical pseudo-Jahn–Teller effect

As indicated in Table III, PJT coupling between states having different characters ($'$versus$''$) with respect to the $\hat{\sigma}_h$ operator can only occur by displacement along an e'' mode. However, many systems of interest, for which JT and PJT couplings are likely, are AB_3 molecules for which no e'' mode exists. For example the A_2'' electronic ground state of NH_3^+ is not coupled to the $\tilde{A}\,E'$ excited state by the e' mode since $A_2''\otimes E'\otimes E'$ does not contain A_1'. However, this picture is only valid if coupling by only a single vibrational mode is considered. In fact, these two states are coupled by simultaneous motions in the a_2'' mode, which pyramidalizes the molecule, and an e' mode because $A_2''\otimes E'\otimes A_2''\otimes E'\supset A_1'$. By allowing nonplanar geometries, the effect of the a_2'' bending can be seen as switching on the PJT coupling caused by displacement along the degenerate e' mode. Thus, this situation can be called a *dynamical* pseudo-Jahn–Teller effect. The electronic Hamiltonian, introducing the coupling due to the umbrella coordinate $Q_{a_2''}$ at first order, is given by

$$\mathcal{H}=\sum_{n=0}^{6}\frac{1}{n!}\{\mathbf{V}_{\mathrm{diag}}^{(n)}+\mathbf{V}_{\mathrm{JT}}^{(n)}+Q_{a_2''}\mathbf{V}_{\mathrm{PJT}}^{(n)}\}+\begin{pmatrix}\mathcal{U}_A & 0 & 0\\ 0 & \mathcal{U}_E & 0\\ 0 & 0 & \mathcal{U}_E\end{pmatrix}. \tag{13}$$

$\mathcal{U}$ are even functions of the umbrella coordinate only and represent the unperturbed potentials of the A and E states along the a_2'' mode. In a multidimensional study of NH_3^+, which is a prototype example for dynamical PJT coupling, such a significant variation of the PJT coupling with the umbrella mode must be taken into account.

IV. APPLICATION

The derived diabatic matrix is applied to the representation of a two-dimensional cut along the e bending mode of the two lowest electronic states of the NH_3^+ cation. These two states correspond to $^2A_2''$ symmetry for the ground state and $^2E'$ symmetry for the excited state. Although the ground state geometry of the cation is trigonal planar, the pyramidal C_{3v} ground state geometry of the neutral NH_3 is chosen as reference geometry for the cuts. In C_{3v} the state symmetries are $^2A_1$ and ^2E. This pyramidal structure is indeed relevant when treating, for example, the ionization process. We also investigated cuts for different pyramidalization angles which influences the strength of the PJT coupling by the discussed dynamical effect. Cuts along the other e vibrational (stretching) mode have also been considered. The presented two-dimensional cut has been found to be the most suitable to perform the following model study.

The reference data for the adiabatic potential energies along the two components of the e bending coordinate are obtained by multireference configuration interaction (MRCI) calculations, using the augmented cc-pVQZ basis set. Since the structure is pyramidalized, the bending angles are defined by the projection of the three N–H bonds onto the plane which is normal to the trisector, i.e., the line that forms equal angles with all three N–H bonds. Using these projected angles, the e coordinates are defined by displacements from the C_{3v} reference geometry as $x=6^{-1/2}(2\Delta\alpha_1-\Delta\alpha_2-\Delta\alpha_3)$ and $y=2^{-1/2}(\Delta\alpha_2-\Delta\alpha_3)$. All calculations have been performed by the MOLPRO program.[24]

The calculated potential cuts show very strong anharmonicity, so that a higher order expansion is necessary to accurately describe the system. In order to decide to which order the expansion has to be done, a stepwise scheme is chosen. We first investigate the influence of the Jahn–Teller coupling order on the description of the potentials, setting the pseudo-Jahn–Teller coupling to zero. To this end, the parameters of the diabatic matrix have to be optimized such that the error between the eigenvalues of the matrix and the *ab initio* energies is minimized. This is achieved by nonlinear least-squares fitting which is performed by a combination of a standard Marquardt–Levenberg procedure embedded into a genetic algorithm.

In Fig. 1 the *ab initio* data are displayed together with the fitting results for the models JT2, JT4, and JT6 along the x coordinate. The notation JTNmax corresponds to expansion up to $n=\mathrm{Nmax}$ for the diagonal $\mathcal{V}^{(n)}$ and Jahn–Teller coupling matrix elements $\mathcal{W}_{JT}^{(n)}$, $\mathcal{Z}_{JT}^{(n)}$ in Eq. (8). In these calculations, all PJT couplings are set to zero. It is immediately evident that the second-order model (JT2) gives very poor results for all three potentials, except for a very narrow region around the reference geometry. The fourth-order approximation (JT4) improves the results drastically, though deviations with respect to the reference data are clearly observable. Finally, the sixth-order expansion (JT6) yields potentials which are virtually indistinguishable from the *ab initio* data.

Though such a good agreement in general is very desirable, one has to keep in mind that in the real system pseudo-

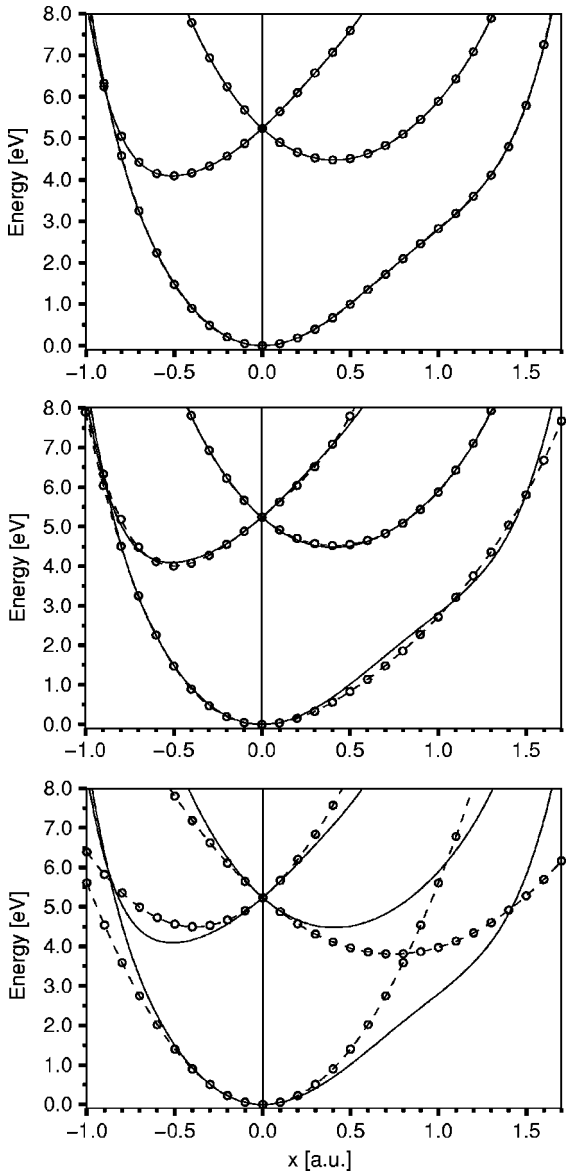

FIG. 1. Adiabatic energies in eV along x for the pure Jahn–Teller models of order 2 (lower panel), 4 (middle panel), and 6 (upper panel) (dashed lines with open circles) compared to the *ab initio* reference data (solid line).

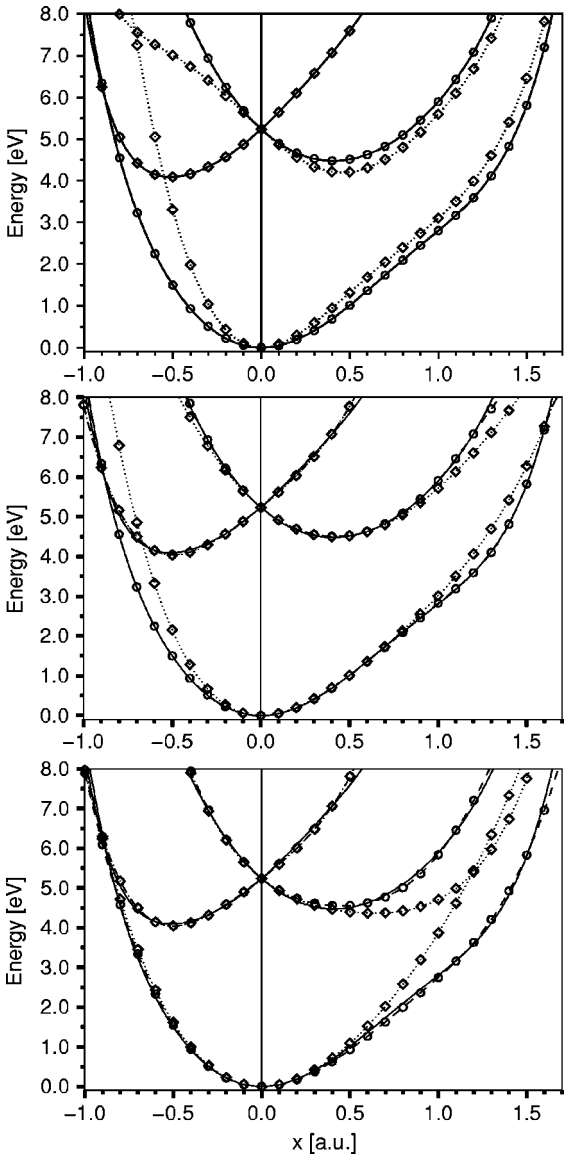

FIG. 2. Adiabatic (dashed lines with open circles) and diabatic (dotted lines with open diamonds) energies in eV along x for JT4/PJT1 (lower panel), JT4/PJT4 (middle pannel), and JT6/PJT6 (upper panel) models compared to the *ab initio* reference data (solid line).

Jahn–Teller coupling also contributes to the shape of the potentials. Thus, the question arises to which degree the anharmonicity has to be accounted for by JT or PJT coupling, respectively. For example, the almost perfect JT6 fit indicates that adding further correction terms by the PJT couplings could render the fitting function too flexible. Thus, the obtained parameters may loose part of their physical significance. In such a case, a careful analysis of the obtained potential matrix, e.g., by using properties of the electronic wave functions, can help to decide about the suitable coupling orders (see below).

We tested all different combinations of JT and PJT coupling and depict characteristic results in Fig. 2. The lower panel of Fig. 2 shows a combination of JT4 and PJT1 which is comparable to the JT4/PJT2 result (not depicted). The adiabatic energies (indicated by dashed lines with open circles) still deviate somewhat from the reference data. Characteristic is that two diabatic energy curves (indicated by dotted lines with open diamonds) cross at a displacement of roughly 1.2 a.u. The middle panel represents the results for the JT4/PJT4 model. The agreement of the adiabatic energies is significantly improved and deviates only very slightly for the E_y state component for negative x (the E_y state component presents a minimum at negative x). The JT4/PJT6 model (not depicted) shows no significant improvement over the JT4/PJT4 combination. However, the JT6/PJT4 model yields almost perfect adiabatic energies while the shape of the diabatic potentials is not qualitatively different from the JT4/PJT4 or JT4/PJT6 results. For these three models, no crossing of the diabatic surfaces at positive x is obtained. As a third example, the JT6/PJT6 model is presented in the upper panel of Fig. 2. The adiabatic energies are now in almost perfect agreement with the reference data. The interesting difference to the other models is that a crossing of diabatic potentials is found at about -0.7 a.u.

It is also helpful to compare the coupling coefficients

TABLE IV. PJT and JT coupling coefficients (a.u.) determined for different models.

	JT2/PJT1	JT4/PJT1	JT4/PJT4	JT6/PJT4	JT4/PJT6	JT6/PJT6
$\lambda_1^{(1)}$ (PJT)	0.0441	0.0548	0.0549	0.1061	0.0467	0.1648
$\lambda_1^{(2)}$ (PJT)			−0.2037	−0.2689	−0.2926	−0.3989
$\lambda_1^{(3)}$ (PJT)			−0.2756	0.1521	0.8040	−0.2183
$\lambda_1^{(4)}$ (PJT)			−0.1482	0.1925	0.2888	0.4670
$\lambda_2^{(4)}$ (PJT)			1.3420	0.3858	1.6040	3.3783
$\lambda_1^{(5)}$ (PJT)					−1.1990	−8.2329
$\lambda_2^{(5)}$ (PJT)					−9.9024	1.7840
$\lambda_1^{(6)}$ (PJT)					7.6403	2.4826
$\lambda_2^{(6)}$ (PJT)					2.4144	−3.7752
$\lambda_1^{(1)}$ (JT)	0.1485	0.1293	0.1337	0.1427	0.1358	0.1433
$\lambda_1^{(2)}$ (JT)	0.0765	−0.1559	−0.1507	−0.0384	−0.1332	0.0347
$\lambda_1^{(3)}$ (JT)		0.6423	0.2933	−0.3355	0.1271	−0.7872
$\lambda_1^{(4)}$ (JT)		1.0700	1.5370	−3.7935	1.4357	1.9497
$\lambda_2^{(4)}$ (JT)		0.5387	0.4516	2.5467	0.7422	−2.3722
$\lambda_1^{(5)}$ (JT)				−1.3896		2.2688
$\lambda_2^{(5)}$ (JT)				7.5791		8.1847
$\lambda_1^{(6)}$ (JT)				97.0116		−13.1908
$\lambda_2^{(6)}$ (JT)				−55.8532		62.5649

obtained for the different models. The values for the PJT and JT couplings for some characteristic cases are collected in Table IV (all parameters are given in atomic units). The linear coupling constant $\lambda_1^{(1)}$ is present in all models and Table IV shows that for all models except JT6/PJT4 and JT6/PJT6 the values are rather similar. It also becomes apparent that the coefficients for the higher couplings are all of significant magnitude. However, one should keep in mind that the factorial factor in Eq. (8) reduces the actual coupling strength for the higher order couplings. Comparison of the higher order parameters shows that the values for different models are in the same order of magnitude but in some cases change sign. Particularly the JT4/PJT6 and JT6/PJT6 values show a significantly different behavior. It is likely that in the JT6/PJT6 case the model is already too flexible to yield parameters of physical significance. This will be illuminated from a different view point in the following.

The fitting error with respect to the adiabatic energies itself is not a suitable measure because JT6/PJT4 and JT6/PJT6 result in comparably small errors. However, the diabatic states vary strongly with the order of the JT and PJT model and thus a criterion is needed to decide which model is relevant. One can obtain useful information from the electronic wave functions of the *ab initio* calculations. The CI vectors of complete active space self-consistent field (CASSCF) or MRCI calculations clearly show whether or not the character of two electronic states is interchanged upon distortion along a given coordinate. A maximum-overlap criterion can be applied to the CASSCF molecular orbitals with respect to a reference wave function in which no coupling of the states in question can occur (e.g., due to symmetry). In the basis of these so-called *diabatic orbitals*, the CI coefficients of the treated states reflect their coupling.[16] The results of such a calculation for displacements along the x coordinate is depicted in Fig. 3.

Since only the $^2A_1$ and ^2E_x state components are coupled along x, it is sufficient to monitor the CI coefficients of the corresponding two main electron configurations. The resulting 2×2 matrix is reorthonormalized and the obtained CI coefficients are plotted against the displacement in x. From this plot it can be seen that the $^2A_1$ and ^2E_x state components start to mix significantly for positive x displacements and to a lesser extent along negative x distortions. However, most important is the finding that apparently no intersection of the configurations is observed. Thus, the two state components keep their main character throughout the whole range of the displacement without a crossing of the diabatic states as well. On the grounds of this analysis it is seen that the best

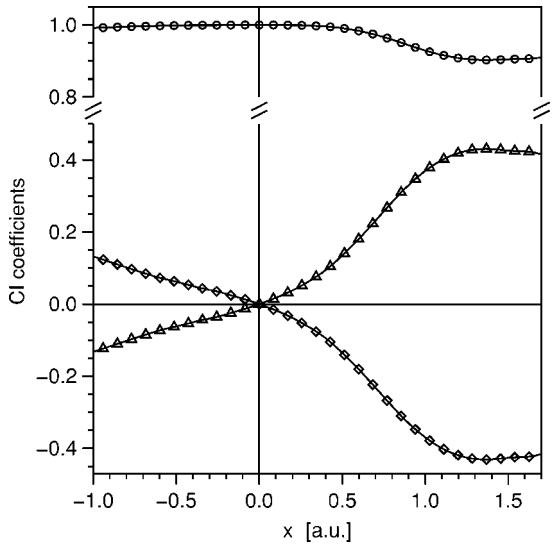

FIG. 3. CI coefficients along x from reorthogonalized 2×2 CI coefficient matrix obtained in the diabatic orbital basis. Main configurations $\ldots(1e_x)^2(1e_y)^2(3a_1)^1$ of $^2A_1$ state and $\ldots(1e_x)^1(1e_y)^2(3a_1)^2$ of ^2E_x state coincide (open circles); contribution of main $^2A_1$ configuration in ^2E_x state (open triangles) and of main ^2E_x configuration in $^2A_1$ state (open diamonds) are antisymmetric.

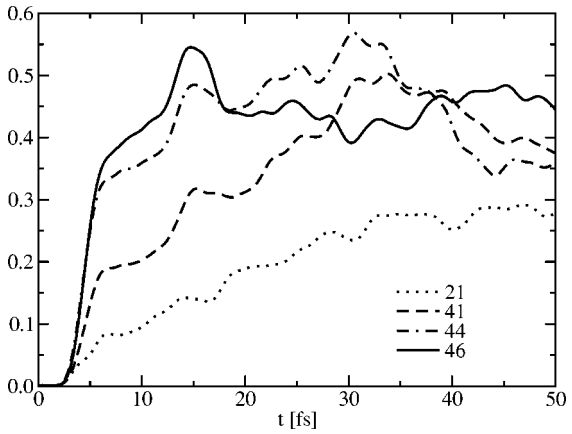

FIG. 4. Adiabatic ground state population as a function of time in femtoseconds for the models JT2/PJT1 (dotted line), JT4/PJT1 (dashed line), JT4/PJT4 (dot-dashed line), and JT4/PJT6 (full line).

representations of the JT and PJT problem for this system, which yield diabatic states in agreement with the above analysis, are obtained from the JT6/PJT4 and JT4/PJT4 combinations. Both models result in similarly small fitting errors.

The effect of the orders of the diabatization scheme on the nuclear dynamics is investigated by wave packet propagations. The dynamics after a vertical excitation onto one of the two excited diabatic surfaces has been studied using a standard propagation scheme based on Fourier transformation. The initial Gaussian wave packet was centered at $(x,y)=(0,0)$ with a width of 40.8 a.u. A constant mass of 1943.38 amu is assumed for the kinetic part of the Hamiltonian, leading to an energy of around 5.6 eV for the wave packet. Figure 4 presents the evolution of the ground state adiabatic electronic population for different orders of the model. Large differences are observed during the first 50 fs with a much slower population transfer to the ground state for the lower PJT order (models JT2/PJT1 and JT4/PJT1). The populations obtained with the higher order models JT4/PJT4 and JT4/PJT6 are similar and only differ in details. For longer propagation time (up to 500 fs), oscillations of the population around 30% for the model 21 and 40% for the other models are observed. The differences obtained for this low dimensionality problem (two vibrational degrees of freedom on three coupled electronic states) indicates that larger differences will be observed for higher dimensional systems because of the increased possibility for the energy to flow from one vibrational mode to another one.

V. CONCLUSION

In this paper, the diabatic Jahn–Teller and pseudo-Jahn–Teller Hamiltonian matrix is presented up to sixth order in both the complex and real representation for a general system with a C_3 symmetry axis. The different possible symmetry groups (D_{3h}, C_{3v}, C_{3h}, and C_3) and coupling mode symmetries (e' and e'') have been investigated. Furthermore, the *dynamical* pseudo-Jahn–Teller effect is discussed. In such a case, the strength of the PJT coupling depends upon distortion along an additional coupling mode.

Application to the representation of a two-dimensional cut of the ground and first exited state of the ammonia cation is presented. Based on the analysis of both the fitting errors to the adiabatic *ab initio* energies and of the evolution of the CI coefficients along the x vibrational coordinate, the combination of Jahn–Teller coupling up to sixth order and pseudo-Jahn–Teller coupling up to fourth order is found to be the most suitable one. It is shown that the higher order JT and PJT expansion developed here can represent the strongly anharmonic potentials of the model system with excellent accuracy. The analysis of dynamical properties and, in particular, of the adiabatic populations underlined the significant role of the coupling order. Application to the NH_3^+ system in full dimensionality is in progress.

ACKNOWLEDGMENTS

The BFHZ-CCUFB is acknowledged for financial support. The authors thank Alexis Viel for checking the calculations. Stefanie Neumann is acknowledged for assistance with the *ab initio* calculations.

[1] H. Köppel, W. Domcke, and L. S. Cederbaum, Adv. Chem. Phys. **57**, 59 (1984).
[2] I. B. Bersuker, *Vibronic Interactions in Molecules and Crystals* (Springer, Berlin, 1989).
[3] H. A. Jahn and E. Teller, Proc. R. Soc. London, Ser. A **161**, 220 (1937).
[4] R. Englman, *The Jahn-Teller Effect in Molecules and Crystals* (Wiley-Interscience, New York, 1972).
[5] *Conical Intersections: Electronic Structure, Dynamics, and Spectroscopy*, edited by W. Domcke, D. R. Yarkony, and H. Köppel (World Scientific, Singapore, 2004).
[6] M. H. Perrin and M. Gouterman, J. Chem. Phys. **46**, 1019 (1967).
[7] J. H. van der Waals, A. M. D. Berghuis, and M. S. de Groot, Mol. Phys. **13**, 301 (1967).
[8] M. Z. Zgierski and M. Pawlikowski, J. Chem. Phys. **70**, 3444 (1979).
[9] H. Köppel, L. S. Cederbaum, and W. Domcke, J. Chem. Phys. **89**, 2023 (1988).
[10] W. Lichten, Phys. Rev. **164**, 131 (1967).
[11] F. T. Smith, Phys. Rev. **179**, 111 (1969).
[12] C. A. Mead and D. G. Truhlar, J. Chem. Phys. **77**, 6090 (1982).
[13] C. A. Mead, J. Chem. Phys. **78**, 807 (1983).
[14] H. Werner and W. Meyer, J. Chem. Phys. **74**, 5802 (1981).
[15] G. Hirsch, R. J. Buenker, and C. Petrongolo, Mol. Phys. **70**, 835 (1990).
[16] W. Domcke and C. Woywod, Chem. Phys. Lett. **216**, 362 (1993).
[17] J. Jensen and D. R. Yarkony, J. Chem. Phys. **89**, 975 (1988).
[18] D. R. Yarkony, Rev. Mod. Phys. **68**, 985 (1996).
[19] T. Pacher, L. S. Cederbaum, and H. Köppel, Adv. Chem. Phys. **84**, 293 (1993).
[20] A. Viel and W. Eisfeld, J. Chem. Phys. **120**, 4603 (2004).
[21] H. C. Longuet-Higgins, Adv. Spectrosc. (N.Y.) **2**, 429 (1961).
[22] M. Döscher, H. Köppel, and P. Szalay, J. Chem. Phys. **117**, 2645 (2002).
[23] The convention used in Ref. 20 is $|\psi_1\rangle=|\psi_x\rangle$ and $|\psi_2\rangle=-|\psi_y\rangle$.
[24] MOLPRO is a package of *ab initio* programs written by H.-J. Werner and P. J. Knowles, with contributions from R. D. Amos, A. Berning, D. L. Cooper *et al.*.